(a)

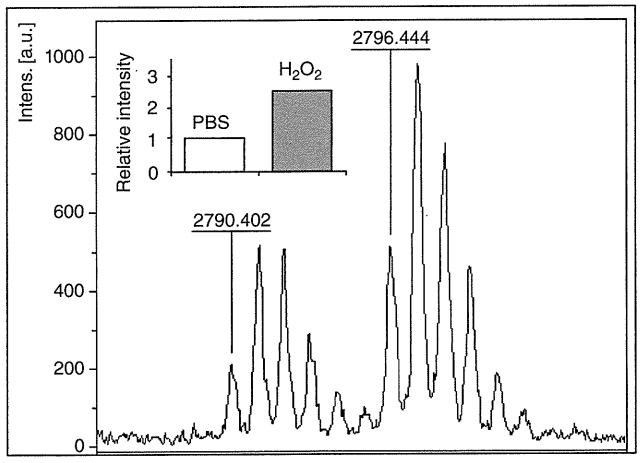

(b)

2790-2796 m/z
FNGGGHINHSIFWTNLSPNGGGEPK
Superoxide dismutase [Mn] mitcondrial precursor (P04179)

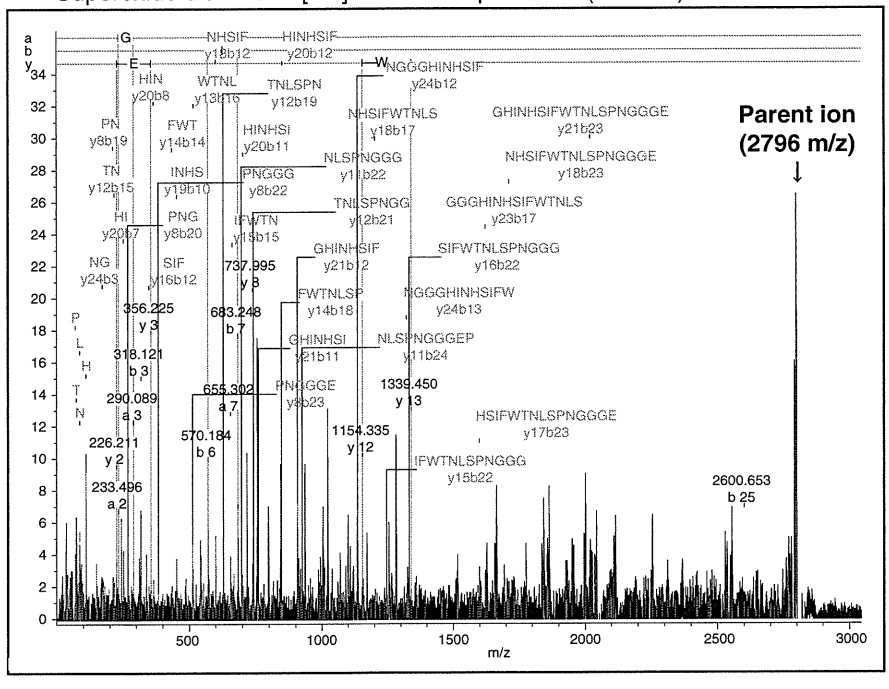

(c)

Western blotting

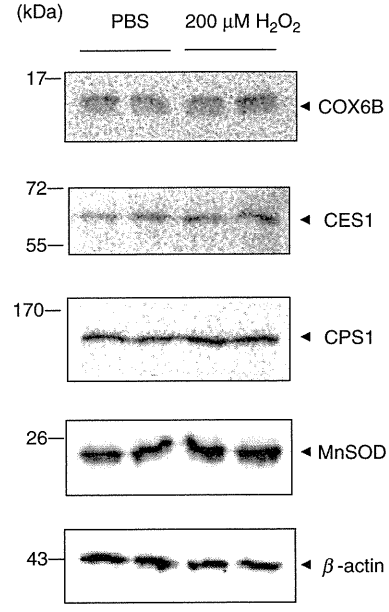

(d)

Densitometric analysis

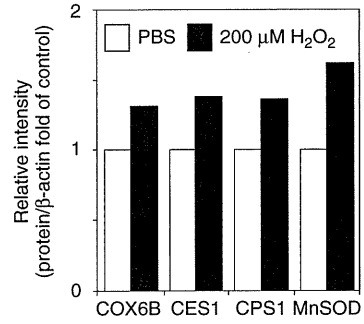

(e)

Real-time RT-PCR

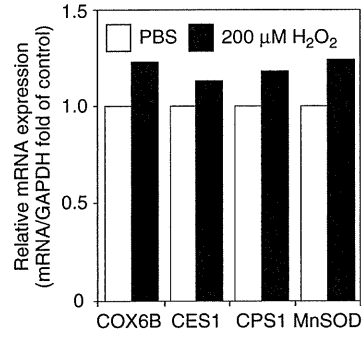

Table 2 Characteristics of study subjects

	Simple steatosis ($n = 15$)	NASH ($n = 29$)	*P*-value
Age (years)	43.2 ± 14.0	60.8 ± 14.9	**<0.001**
Sex (male/female)	11/4	11/18	**<0.05**
Height (cm)	162.5 ± 11.2	156.5 ± 8.7 (28)	0.05
Bodyweight (kg)	69.3 ± 11.8	69.2 ± 15.2 (28)	0.58
BMI (kg/m^2)	26.3 ± 3.6	28.1 ± 4.4 (28)	0.23
Diabetes (yes/no)	5/10	13/15 (28)	0.52
Hyperlipidemia (yes/no)	10/5	16/12 (28)	0.74
Hypertension (yes/no)	4/11	10/18 (28)	0.74
Hb (g/dL)	15.1 ± 1.8	14.4 ± 1.5	0.07
Plt (×10^4/μL)	23.8 ± 7.5	18.8 ± 7.0	**<0.05**
AST (IU/L)	41.6 ± 20.2	69.4 ± 46.5	**<0.05**
ALT (IU/L)	83.1 ± 53.1	94.6 ± 96.0	0.89
γ-GTP (U/L)	75.3 ± 52.4	155.6 ± 303.1	0.40
ChE (IU/L)	417.9 ± 97.5	352.8 ± 135.5	**<0.05**
γ-Glob (g/dL)	1.27 ± 0.40	1.50 ± 0.44 (24)	0.06
Total cholesterol (mg/dL)	209.2 ± 45.8	204.8 ± 52.1	0.97
Triglyceride (mg/dL)	168.3 ± 65.8	184.8 ± 168.3	0.45
BS (mg/dL)	119.1 ± 48.5	112.3 ± 34.3	0.61
Ferritin (mg/dL)	190.0 ± 112.7 (14)	239.8 ± 234.3 (22)	0.75

Values represent means ± standard deviation for the indicated number of subjects. Significant differences between the mean values ($P < 0.05$) were assessed by Fisher's exact probability test (sex, diabetes, hyperlipidemia and hypertension) or Mann–Whitney's *U*-test (other items).
Values in parentheses indicate the number of samples. Bold characters highlight statistically significant *P*-values.
ALT, alanine aminotransferase; AST, aspartate aminotransferase; BMI, body mass index; BS, blood sugar; ChE, choline esterase; γ-Glob, γ-globulin; γ-GTP, γ-glutamyl transpeptidase; Hb, hemoglobin; NASH, non-alcoholic steatohepatitis; Plt, platelet count.

The clinical characteristics of the SS and NASH groups were not significantly different except for the average age, platelet count (Plt), aspartate aminotransferase (AST) and choline esterase (ChE) (Table 2). We examined the serum MnSOD levels in healthy subjects ($n = 20$), SS patients ($n = 15$) and NASH patients ($n = 29$). There were no significant differences in MnSOD serum levels between healthy subjects and SS patients (Fig. 2a). In contrast, NASH patients had significantly higher serum MnSOD levels than both healthy subjects and SS patients (Fig. 2a). In addition, as shown in Figure 2(b), the serum levels of MnSOD tended to increase in parallel with the fibrosis stage. In contrast, there was no correlation between the levels of MnSOD and the activity grade of NASH (Fig. 2c). ROC of MnSOD levels were constructed to distinguish NASH (29 patients) from SS (15 patients) (Fig. 2d). The serum MnSOD threshold level that was used to predict NASH was calculated to be 71.8 ng/mL. At this threshold, the sensitivity was 69.0% and the specificity was 80.0%. The area under the ROC (AUC) for serum MnSOD levels was 0.760 ($P = 0.010$). The ROC curves for Plt, AST and ChE, which were significantly different between SS and NASH (Table 2), were also constructed. As a result, the AUC (*P*-value, threshold, sensitivity [%], specificity [%]) for Plt, serum AST and ChE were 0.733 (0.012, 19.4, 65.5, 86.7), 0.726 (0.015, 42.0, 65.5, 73.3) and 0.687 (0.044, 317.5, 48.3, 86.7), respectively.

DISCUSSION

IN THIS REPORT, we used the NBS labeling method to identify novel oxidative stress markers in hepatocytes that can be used as diagnostic markers for NASH and identified four candidate markers, COX6B, CES1, CPS1 and MnSOD, that were upregulated with H_2O_2 loading (Table 1, Fig. 1). Several recent studies have reported novel approaches that combine the NBS labeling method with 2-DE, high-performance liquid chromatography (HPLC) and lectin column chromatographic techniques.[13–16] In our present study, we identified only four proteins, indicating that it may be necessary to modify the current method by 2-DE and column chromatographic techniques to identify additional NBS-

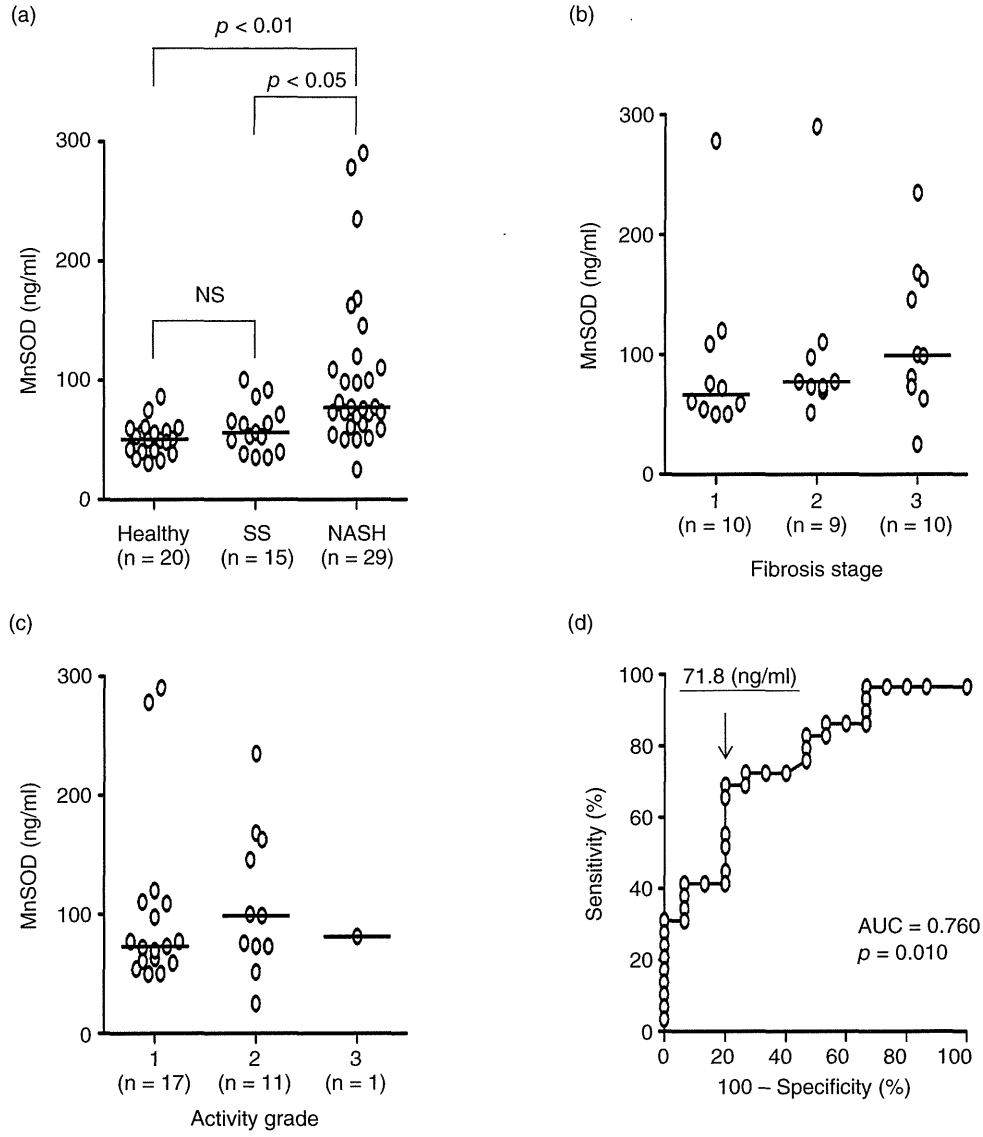

Figure 2 Clinical significance of serum MnSOD levels. (a) Serum MnSOD levels in healthy subjects and patients with SS or non-alcoholic steatohepatitis (NASH). Serum MnSOD levels were measured by enzyme-linked immunosorbent assay. (b) Comparison between serum MnSOD levels and the fibrosis stage in SS and NASH patients. (c) Comparison between serum MnSOD levels and the activity grade in SS and NASH patients. (d) Receiver–operator curve for MnSOD. The differences among three groups were evaluated using Kruskal–Wallis test followed by Dunn's multiple comparison test. Correlation coefficients were calculated by Spearman's rank correlation analysis. Bars indicate the median in the respective groups. AUC, area under the curve.

labeled peptides. In addition, further studies are needed to identify novel biomarkers by other proteomic techniques using serum samples from SS and NASH patients.

COX6B, CPS1 and MnSOD are mitochondrial proteins, and therefore may be indicators of mitochondrial disorders that are induced by oxidative stress. CPS1 is expressed primarily in the liver and small intestine and is involved in the urea cycle.[17] In galactosamine-induced rat acute hepatitis, plasma concentrations of CPS1 increase up to approximately 100-fold for 24 h after treatment.[18] This may indicate that secreted CPS1 is a serum marker for acute hepatitis. CES1, which is responsible for detoxification of exogenous compounds such

as esters, amides and thioesters, is also known to exist in the serum. Therefore, CES1, like CPS1, may be a serum oxidative stress marker.[19,20] Additional studies are needed to further evaluate the serum levels of these identified proteins.

MnSOD primarily exists in the mitochondrial matrix and eliminates reactive oxygen species (ROS) by catalyzing the dismutation of superoxide radicals and hydrogen peroxide.[19] Furthermore, MnSOD expression was previously shown to increase after exposure to hydrogen peroxide in rat hepatocytes.[21] In addition, obese mice were previously reported to have increased hepatic H_2O_2 levels and necrosis following an imbalance between increased MnSOD, which forms H_2O_2, and decreased glutathione activity, which detoxifies H_2O_2.[22] We found that MnSOD is potentially a novel diagnostic marker of NASH that can be used to distinguish between SS and NASH. One of the mechanisms contributing to increased MnSOD serum levels in NASH might be the discharge of MnSOD from necrotic hepatocytes. On the other hand, in the liver, several pro-inflammatory cytokines, such as tumor necrosis factor-α, interleukin-6 and interleukin-1β can act as common inducers of NASH.[23,24] Such pro-inflammatory cytokines have been shown to induce MnSOD expression in liver tissues.[25] Furthermore, pro-inflammatory cytokines induced the expression and secretion of MnSOD in several cancer cell lines including hepatoma cells.[26,27] In our present study, the origin of MnSOD produced in NASH and the precise mechanism of increased serum levels of MnSOD in NASH patients remain unclear. However, these reports may partially support the mechanism of MnSOD production in NASH. Further elucidation is necessary to clarify the mechanism of MnSOD expression and production in NASH.

Several reports have shown a relationship between the enzymatic activity of MnSOD and non-alcoholic fatty liver disease, NASH, liver cirrhosis and hepatocellular carcinoma.[28–31] Ono *et al.* showed that MnSOD serum levels were significantly increased in patients with primary biliary cirrhosis compared to patients with other liver diseases.[32] However, the serum protein levels of MnSOD in liver diseases have not been fully evaluated. In addition, the enzymatic activity of serum MnSOD was not different among the three groups and this activity did not correlate with serum MnSOD levels in our study (data not shown). The reasons for these results are unclear. However, as shown in Figure 2(b), serum MnSOD levels increased in parallel with the stage of fibrosis in NASH. The increase in serum MnSOD levels also significantly correlated with the serum AST levels (data not shown). These results indicate that serum MnSOD might be a biomarker that reflects hepatitic and fibrotic pathology. In addition, although MnSOD levels should increase in patients with other diseases including CHC, ROC analysis revealed that serum MnSOD may be a more sensitive biomarker than Plt, AST and ChE. We concluded that serum MnSOD is a useful biomarker that can distinguish SS and NASH.

ACKNOWLEDGMENTS

THIS WORK WAS supported in part by Grants-in-Aid for Scientific Research (C) from the Japan Society for the Promotion of Science (JSPS), Research for Promoting Technological Seeds (A) from the Japan Science and Technology Agency (JST), the Collaboration of Regional Entities for the Advancement of Technological Excellence (CREATE) from the JST, and a Grant-in-Aid (Research on Hepatitis and BSE) from the Ministry of Health, Labor and Welfare of Japan.

REFERENCES

1 Leclercq IA, Farrell GC, Field J, Bell DR, Gonzalez FJ, Robertson GR. CYP2E1 and CYP4A as microsomal catalysts of lipid peroxides in murine nonalcoholic steatohepatitis. *J Clin Invest* 2000; **105**: 1067–75.
2 Piccoli C, Scrima R, D'Aprile A *et al.* Mitochondrial dysfunction in hepatitis C virus infection. *Biochim Biophys Acta* 2006; **1757**: 1429–37.
3 Perez-Carreras M, Del Hoyo P, Martin MA *et al.* Defective hepatic mitochondrial respiratory chain in patients with nonalcoholic steatohepatitis. *Hepatology* 2003; **38**: 999–1007.
4 Wu LL, Chiou CC, Chang PY, Wu JT. Urinary 8-OHdG: a marker of oxidative stress to DNA and a risk factor for cancer, atherosclerosis and diabetics. *Clin Chim Acta* 2004; **339**: 1–9.
5 Fujii J, Taniguchi N. Phorbol ester induces manganese-superoxide dismutase in tumor necrsis factor-resistant cells. *J Biol Chem* 1991; **266**: 23142–6.
6 Nishinaka Y, Masutani H, Nakamura H, Yodoi J. Regulatory roles of thioredoxin in oxidative stress-induced cellular responses. *Redox Rep* 2001; **6**: 289–95.
7 Kuyama H, Watanabe M, Toda C, Ando E, Tanaka K, Nishimura O. An approach to quantitative proteome analysis by labeling tryptophan residues. *Rapid Commun Mass Spectrom* 2003; **17**: 1642–50.
8 Matsuo E, Toda C, Watanabe M *et al.* Improved 2-nitrobenzenesulfenyl method: optimization of the protocol and improved enrichment for labeled peptides. *Rapid Commun Mass Spectrom* 2006; **20**: 31–8.

9 Lanford RE, Carey KD, Estlack LE, Smith GC, Hay RV. Analysis of plasma protein and lipoprotein synthesis in long-term primary cultures of baboon hepatocytes maintained in serum-free medium. *In Vitro Cell Dev Biol* 1989; **25**: 174–82.
10 Rosseland CM, Wierod L, Oksvold MP *et al.* Cytoplasmic retention of peroxide-activated ERK provides survival in primary cultures of rat hepatocytes. *Hepatology* 2005; **42**: 200–7.
11 Conde de la Rosa L, Schoemaker MH, Vrenken TE *et al.* Superoxide anions and hydrogen peroxide induce hepatocyte death by different mechanisms: involvement of JNK and ERK MAP kinases. *J Hepatol* 2006; **44**: 918–29.
12 Matsuo E, Toda C, Watanabe M *et al.* Selective detection of 2-nitrobenzenesulfenyl-labeled peptides by matrix-assisted laser desorption/ionization-time of flight mass spectrometry using a novel matrix. *Proteomics* 2006; **6**: 2042–9.
13 Sumida Y, Nakashima T, Yoh T *et al.* Serum thioredoxin levels as a predictor of steatohepatitis in patients with non-alcoholic fatty liver disease. *J Hepatol* 2003; **38**: 32–8.
14 Ou K, Kesuma D, Ganesan K *et al.* Quantitative profiling of drug-associated proteomic alterations by combined 2-nitrobenzenesulfenyl chloride (NBS) isotope labeling and 2DE/MS identification. *J Proteome Res* 2006; **5**: 2194–206.
15 Iida T, Kuyama H, Watanabe M *et al.* Rapid and efficient MALDI-TOF MS peak detection of 2-nitrobenzenesulfenyl-labeled peptides using the combination of HPLC and an automatic spotting apparatus. *J Biomol Tech* 2006; **17**: 333–41.
16 Ueda K, Katagiri T, Shimada T *et al.* Comparative profiling of serum glycoproteome by sequential purification of glycoproteins and 2-nitrobenzensulfenyl (NBS) stable isotope labeling: a new approach for the novel biomarker discovery for cancer. *J Proteome Res* 2007; **6**: 3475–83.
17 Pearson DL, Dawling S, Walsh WF *et al.* Neonatal pulmonary hypertension–urea-cycle intermediates, nitric oxide production, and carbamoyl-phosphate synthetase function. *N Engl J Med* 2001; **344**: 1832–8.
18 Ozaki M, Terada K, Kanazawa M, Fujiyama S, Tomita K, Mori M. Enzyme-linked immunosorbent assay of carbamoylphosphate synthethase 1: plasma enzyme in rat experimental hepatitis and its clearance. *Enzyme Protein* 1994–1995; **48**: 213–21.
19 Munger JS, Shi GP, Mark EA, Chin DT, Gerard C, Chapman HA. A serine esterase released by human alveolar macrophages is closely related to liver microsomal carboxylesterases. *J Biol Chem* 1991; **266**: 18832–8.
20 Yan B, Yang D, Bullock P, Parkinson A. Rat serum carboxylesterase. Cloning, expression, regulation, and evidence of secretion from liver. *J Biol Chem* 1995; **270**: 19128–34.
21 Kurobe N, Inagaki T, Kato K. Sensitive enzyme immunoassay for Mn superoxide dismutase. *Clin Chim Acta* 1990; **192**: 171–9.
22 Rohrdanz E, Kahl R. Alterations of antioxidant enzyme expression in response to hydrogen peroxide. *Free Radic Biol Med* 1998; **24**: 27–38.
23 Robin MA, Demeilliers C, Sutton A *et al.* Alcohol increases tumor necrosis factor a and decreases nuclear factor kB to activate hepatic apoptosis in genetically obese mice. *Hepatology* 2005; **42**: 1280–90.
24 Hotamisligil GS. Inflammation and metabolic disorders. *Nature* 2006; **444**: 860–7.
25 Shoelson SE, Lee J, Goldfine AB. Inflammation and insulin resistance. *J Clin Invest* 2006; **116**: 1793–801.
26 Sato M, Sasaki M, Hojo H. Antioxidative roles of metallothionein and manganese superoxide dismutase induced by tumor necrosis factor-α and interleukin-6. *Arch Biochem Biophys* 1995; **316**: 738–44.
27 Ono M, Kohda H, Kawaguchi T *et al.* Induction of Mn-superoxide dismutase by tumor necrosis factor, interleukin-1 and interleukin-6 in human hepatoma cells. *Biochem Biophys Res Commun* 1992; **182**: 1100–7.
28 Nakata T, Suzuki K, Fujii J, Ishikawa M, Taniguchi N. Induction and release of manganese superoxide dismutase from mitochondria of human umbilical vein endothelial cells by tumor necrosis factor-α and interleukin-1β. *Int J Cancer* 1993; **55**: 646–50.
29 Videla LA, Rodrigo R, Orellana M *et al.* Oxidative stress-related parameters in the liver of non-alcoholic fatty liver disease patients. *Clin Sci* 2004; **106**: 261–8.
30 Clemente C, Elba S, Buongiorno G *et al.* Manganese superoxide dismutase activity and incidence of hepatocellular carcinoma in patients with Child–Pugh class A liver cirrhosis: 7-year follow-up study. *Liver Int* 2007; **27**: 791–7.
31 Perlemuter G, Davit-Spraul A, Cosson C *et al.* Increase in liver antioxidant enzyme activities in non-alcoholic fatty liver disease. *Liver Int* 2005; **25**: 946–53.
32 Ono M, Sekiya C, Ohhira M *et al.* Elevated level of serum Mn-superoxide dismutase in patients with primary biliary cirrhosis: possible involvement of free radicals in the pathogenesis in primary biliary cirrhosis. *J Lab Clin Med* 1991; **118**: 476–83.

J Gastroenterol (2010) 45:459–467
DOI 10.1007/s00535-009-0160-5

ORIGINAL ARTICLE—LIVER, PANCREAS, AND BILIARY TRACT

The complement component C3a fragment is a potential biomarker for hepatitis C virus-related hepatocellular carcinoma

Shuji Kanmura · Hirofumi Uto · Yuko Sato · Koutarou Kumagai · Fumisato Sasaki · Akihiro Moriuchi · Makoto Oketani · Akio Ido · Kenji Nagata · Katsuhiro Hayashi · Sherri O. Stuver · Hirohito Tsubouchi

Received: 1 July 2009 / Accepted: 28 October 2009 / Published online: 9 December 2009

Abstract
Background Hepatocellular carcinoma (HCC) has a high mortality rate, and early detection of HCC improves patient survival. However, the molecular diagnostic markers for early HCC have not been fully elucidated. The aim of this study was to identify novel diagnostic markers for HCC.
Methods Serum protein profiles of 45 hepatitis C virus infection (HCV)-related HCC patients (HCV-HCC) were compared to 42 HCV-related chronic liver disease patients without HCC (HCV-CLD) and 21 healthy volunteers using the ProteinChip SELDI system. One of the identified proteins was evaluated as a diagnostic marker for HCC in patients with HCV.
Results Five protein peaks (4067, 4470, 7564, 7929, and 8130 m/z) had p-values less than 1×10^{-7} and were significantly increased in the sera of HCV-HCC patients compared to HCV-CLD patients and healthy volunteers. Among these proteins, an 8130 m/z peak was the most differentially expressed and identified as the complement component 3a (C3a) fragment. For HCV-HCC and HCV-CLD, the relative intensity of this C3a fragment had the best area under the ROC curve [0.70], followed by des-γ-carboxy prothrombin (DCP) [0.68], lectin-bound alpha fetoprotein (AFP-L3) [0.58] and AFP [0.53] for HCC. A combined analysis of the C3a fragment, AFP and DCP led to a 98% positive identification rate. In addition, the measurable C3a fragment in some HCC patients was not only significantly higher in the year of HCC onset compared to the pre-onset year, but also decreased after treatment.
Conclusions The 8130 m/z C3a fragment is a potential marker for the early detection of HCV-related HCC.

Keywords Hepatocellular carcinoma · Complement component C3a · Serum proteomics · Serum biomarkers · Proteinchip SELDI system · Hepatitis C virus

S. Kanmura · H. Uto (✉) · K. Kumagai · F. Sasaki · A. Moriuchi · M. Oketani · A. Ido · H. Tsubouchi
Digestive Disease and Life-style Related Disease Health Research, Human and Environmental Sciences, Kagoshima University Graduate School of Medical and Dental Sciences, 8-35-1 Sakuragaoka, Kagoshima 890-8520, Japan
e-mail: hirouto@m2.kufm.kagoshima-u.ac.jp

Y. Sato
Miyazaki Prefectual Industrial Support Foundation, Miyazaki, Japan

K. Nagata
Division of Gastroenterology and Hematology, Internal Medicine, Faculty of Medicine, University of Miyazaki, Miyazaki, Japan

K. Hayashi
Faculty of Medicine, Center for Medical Education, University of Miyazaki, Miyazaki, Japan

S. O. Stuver
Department of Epidemiology, Boston University School of Public Health, Boston, MA, USA

S. O. Stuver
Department of Epidemiology, Harvard School of Public Health, Boston, MA, USA

Introduction

Hepatocellular carcinoma (HCC) is reportedly the third most frequent cause of global cancer-related deaths, and the incidence of HCC is increasing worldwide [1, 2]. The clearly established risk factor for HCC is chronic hepatitis C virus (HCV) infection [3].

To date, both ultrasonography and serum tumor markers such as the alpha fetoprotein (AFP), and des-γ-carboxy prothrombin (DCP) assay are the principle methods for screening and detecting HCC. Routine screening is the best method to detect early HCC and improve patient survival; however, elevated serum AFP and DCP levels have insufficient sensitivity and specificity, respectively. The sensitivity and specificity of serum elevated AFP levels were reported to range from 39–64% and 76–91%, while those of the serum elevated DCP levels were 41–77% and 72–98%, respectively [4–9]. In addition, it was recently reported that only a small percentage of small HCC tumors were diagnosed based on AFP and DCP [6, 10]. The lens culinaris agglutinin-reactive fraction of AFP (lectin-bound AFP or AFP-L3) has been reported to be elevated in the serum of HCC patients. Although AFP-L3 has a high range of specificity for detecting HCC, the sensitivity is low [11, 12]. The ability to detect early HCC, prior to the onset of clinical symptoms, leads to curative treatment and significantly improves the disease prognosis. Thus, additional biochemical markers are necessary for the specific detection of early HCC.

Serum profiling using a proteomic approach is thought to be a useful technique to detect or predict early HCC in chronic liver disease patients. Studies using the ProteinChip SELDI system, which is a powerful tool to discover new biomarkers, have shown that this method may be successfully used to diagnose HCC. Zinkin et al. [13], Schwegler et al. [14] and our research group [15] previously detected early HCC using the profile of several protein peaks that were identified by the ProteinChip SELDI system. Paradis et al. [16] reported the highest discriminating peak (8900 Da), which was identified as the V10 fragment of vitronectin. Furthermore, Lee et al. [17] described complement 3a, which had a molecular weight of approximately 8900 Da, as a novel marker of HCC. Therefore, using this proteomic approach to identify specific proteins may not only help establish simple methods to detect HCC, but also further our understanding of the molecular mechanisms of hepatocarcinogenesis and facilitate the development of novel cancer therapies. Therefore, this study assessed and compared the protein expression profiles in the sera of HCC patients in order to identify a more useful biomarker of HCC-associated HCV infection using proteomic approach.

Materials and methods

Samples

Eighty-seven patients [45 HCC patients and 42 patients with chronic liver diseases without HCC (CLD)] with HCV infection were selected to participate in this study (Table 1). These patients provided informed consent. Serum samples were collected by the Faculty of Medicine, University of Miyazaki (Miyazaki, Japan), and some patients were in a hyperendemic HCV area with a cohort study in Miyazaki [18]. The sera of all patients with and without HCC, which was confirmed by abdominal ultrasonography or computed tomography, were obtained prior to treatment. All of the sera samples from HCV-infected patients were analyzed in a previous study [15]. In addition, sera from 10 HCV-HCC patients who were diagnosed with HCC within 1 or 2 years and sera from five patients who had received radiofrequency ablation (RFA), percutaneous ethanol injection therapy (PEIT) and/or transarterial chemoembolization (TACE) for HCC were collected through a cohort study in Miyazaki. We also analyzed the sera of 21 healthy volunteers without HCC as controls. After freezing and thawing once, all samples were separated into 50–100 μl aliquots and refrozen at −80°C. The study protocol was approved by the Ethics Committee of the Faculty of Medicine, University of Miyazaki, Kagoshima University Graduate School of Medical and Dental Sciences, and Harvard School of Public Health and Boston University School of Public Health.

Table 1 Patient characteristics

	HCC[a]	CLD[b]	*p* value
Patients (male/female)	45 (40/5)	42 (40/2)	–
Age	73.6 [63–85]	61.8 [41–83]	<0.0001
PLT[c] ($\times 10^4$/ul)	12.5 ± 5.8	8.4 ± 4.6	0.001
Albumin (g/dl)	3.8 ± 0.8	4.2 ± 1.6	0.8
ALT[d] (IU/l)	57.7 ± 28.3	52.8 ± 37.5	0.7
AFP[e] (ng/ml)	311 ± 1144	51.6 ± 36.1 (38)	0.008
DCP[f] (mAU/ml)	235 ± 605 (44)	37.1 ± 59.8 (39)	<0.0001
HA[g] (ng/ml)	388 ± 446 (40)	280 ± 272 (27)	0.6
Diameter of HCC (mm)	23.2 [10–40]	–	–
TNM stage[h] (I/II/III/IV)	24/18/3/0	–	–

Data are shown as the means ± SD or means [range] (numbers)

[a] Hepatocellular carcinoma

[b] Chronic liver disease

[c] Platelet counts

[d] Alanine aminotransferase

[e] Alpha fetoprotein

[f] Des-γ-carboxy prothrombin

[g] Hyaluronic acid

[h] TNM; primary tumor/lymph node/distant metastasis

SELDI-TOF/MS analysis of sera

Expression difference mapping analysis profiles of the samples were obtained using weak cation-exchange (CM10) ProteinChip Arrays (Bio-Rad Laboratories). Arrays were analyzed by ProteinChip reader as previously reported [15]. In addition, the laser intensity ranged from 220 to 245, with a detector sensitivity of 8, and spectra ranging from 1300 to 150000 m/z were selected for analysis in this study.

Separation of candidate biomarker (8.1 k m/z)

The purification strategy was determined by the ProteinChip Arrays. Two hundred microliters of sera from HCV-HCC patients were diluted 5-fold into 50 mM Na-phosphate buffer, pH 7.0, and loaded onto a CM-Ceramic HyperD F spin column (Bio-Rad Laboratories). After equilibrating with the same buffer, the samples were eluted with a stepwise sodium chloride gradient from 0, 200, 300, and 1000 mM. The elution was desalinated and concentrated using a centrifugal concentrator (VIVASPIN, Vivascience, Hannover, Germany), and the purification progress was monitored using NP20 arrays. The flow-through fraction was dialyzed and then separated by 16.5% tricine one-dimensional sodium dodecyl sulfate–polyacrylamide gel electrophoresis (SDS–PAGE). The SDS–PAGE samples were run in tricine sodium dodecyl sulfate buffer according to the manufacturer's instructions and then stained with Coomassie brilliant blue (CBB).

Identification of the candidate biomarker (8.1 k m/z)

Gel pieces containing the target 8.1 k m/z protein were excised. The excised bands were reduced and alkylated for 30 min at room temperature, and then digested with trypsin (Modified Sequence Grade, Roche Diagnostics, Basel, Switzerland) in Tris–HCl, pH 8.0, for 20 h at 35°. The reaction solution was applied to NP20 arrays and allowed to air dry. To identify the protein, the digested peptides were purified by high-performance liquid chromatography (HPLC; MAGIC 2002; Michrom Bioresources Inc., Auburn, CA) and analyzed by Q-Tof2 (Micromass; Waters Ltd., Hertsfordshire, UK). The HPLC solvent consisted of solvent A (2% acetonitlile/0.1% formic acid) and B (90% acetonitlile/0.1% formic acid). The digested peptides were separated with a linear gradient from 10 to 50% solvent B with a flow rate of 400 nl/min using HPLC [19]. Mass spectral data were searched with Mascot (http://www.matrixscience.com) to identify proteins based on the peptide mass [20, 21].

Immunodepletion assay

For immunodepletion, serum samples were prepared as follows. Sera (250 μl) from HCC patients were diluted 5-fold in 50 mM Tris–HCl buffer, pH 8.0, and loaded onto a CM-Sepharose Fast Flow spin column (GE Healthcare Bio-Sciences Corp., NJ). After equilibration with the same buffer, the samples were eluted with a stepwise sodium chloride gradient from 0, 500, and 1000 mM. The elution from each NaCl concentration was monitored using NP20 arrays. To prepare the antibodies for immunodepletion, 6 μl anti-human C3 antibody, which detected C3 and C3a expression, or anti-C4a antibody (Santa Cruz Biotechnology, Santa Cruz, CA) was incubated with 20 μl Interaction Discovery Mapping (IDM) affinity beads (Bio-Rad Laboratories) and Protein A (Sigma Chemical Co, St. Louis, MO) over night at 4° with shaking. These beads were centrifuged, and the supernatant was discarded. The beads were washed with 50 mM phosphate buffer (pH 7.0), and 3 μl of the prepared serum sample was incubated with 15 μl IDM affinity beads with shaking for 2 h at 4°. As a negative control, 3 μl sample was incubated with IDM affinity beads and Protein A with an anti-C4a antibody or without antibody. After the incubation, the samples were cleared by centrifugation, and 5 μl of each supernatant was analyzed on NP20 ProteinChip arrays in a PBS II reader.

Cell culture and SELDI-TOF/MS analysis of culture supernatants

The human hepatocarcinoma cell line HuH-7 and human hepatoblastoma cell line HepG2 were cultured in Dulbecco's modified Eagle's medium supplemented with 10% fetal bovine serum (FBS), 100 IU/ml penicillin G, and 100 mg/ml streptomycin sulfate (Invitrogen, Carlsbad, CA). Before starting the experiments, the cells were cultured on 96-well microplates in medium without FBS for 24 h. After washing with FBS-free media, the cells were cultured for 24 h with FBS-free media with or without 500 μg/ml of C3a (Calbiochem, San Diego, CA). The supernatants were collected by centrifugation and analyzed for the expression of 8.1 k m/z using the ProteinChip system.

Statistical analysis

Values are shown as the means ± SD. Statistical differences, including laboratory data and individual peaks in SELDI TOF/MS, were determined using the Mann–Whitney U test. Values of $p < 0.05$ were considered statistically significant. The discriminatory power for each putative marker was described via receiver operating characteristics

(ROC) area under the curve (AUC). These statistical analyses were performed using STATVIEW 4.5 software (Abacus Concepts, Berkeley, CA), SPSS software (SPSS Inc., Chicago, IL), JMP software, or Ciphergen ProteinChip Software, version 3.0.2.

Results

Profiling sera from HCC patients and healthy controls

We analyzed the sera of all patients with HCV-HCC or HCV-CLD and healthy controls without HCC using the CM10 ProteinChip array to identity the most differential protein peak. Peaks were automatically detected using the Ciphergen ProteinChip Software 3.0.2. following baseline subtraction as described previously [15, 22]. This analysis identified 178 protein peak clusters, as seen in the spectrum representations from the three groups (HCV-HCC, HCV-CLD, and healthy control) in the 3000- to 15000-m/z range. Peak expressions were increased for 18 proteins and decreased for 14 proteins in sera from HCV-HCC patients compared to HCV-CLD patients. Compared to healthy subjects, 68 protein peaks were increased, and 16 protein peak intensities were decreased in the sera of HCV-HCC patients. Five protein peaks (4067, 4470, 7564, 7929, and 8130 m/z) had a p-value less than 1×10^{-7} and were significantly increased in the sera of HCC patients compared to the sera of HCV-CLD patients and healthy volunteers. In particular, an 8130 m/z peak was the most significantly different peak and had the most differential expression profile between patients with HCV-HCC and with HCV-CLD.

Purification and identification of the 8.1 k m/z peak

We optimized the adsorption and desorption conditions on the arrays using an HCV-HCC patient serum sample and healthy volunteer serum sample in order to determine a procedure to purify the target 8.1 k m/z protein. The optimal pH for retention of the 8.1 k m/z protein was a *pI* value of approximately 7.0 on the CM10 arrays, which indicates that weak cation-exchange sorbents and buffer pH should be fixed for further experiments. The target protein was eluted by increasing the sodium chloride concentrations in a Na-phosphate buffer and was eluted in the 1000 mM sodium chloride fraction. The concentrated serum protein that was eluted with 1000 mM sodium chloride was applied to SDS–PAGE for further separation. The 8.1 k m/z protein was identified and excised by in-gel trypsin digestion for identification. The peptide sequences were analyzed using liquid chromatography (LC)-MS/MS and then examined by a database search with Mascot. The digested peptides matched human complement C3a (Fig. 1).

After reacting the HCC sera with anti-complement C3a or anti-C4 antibodies or without antibody, the supernatants were analyzed by the SELDI ProteinChip system for immunodepletion. Analysis of the supernatant showed that only the 8.1 k m/z peak corresponding to complement C3a

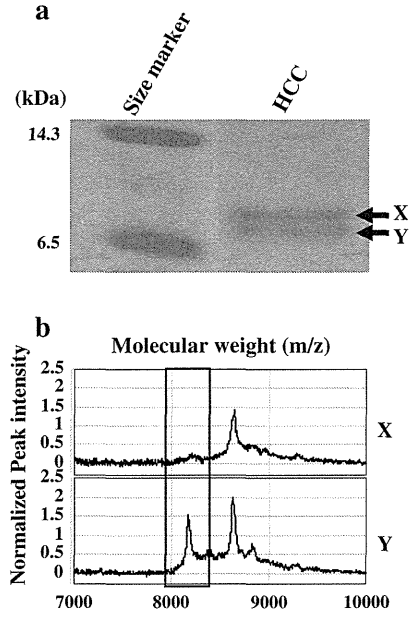

c Complement component 3:
Total score: 70, Peptides matched: 2

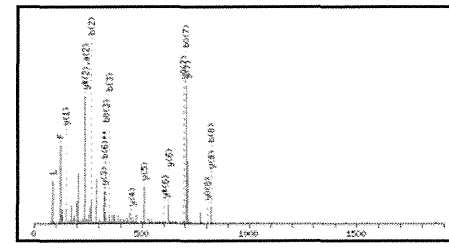

FISLGEACK , Start – End Sequence: 713 - 721

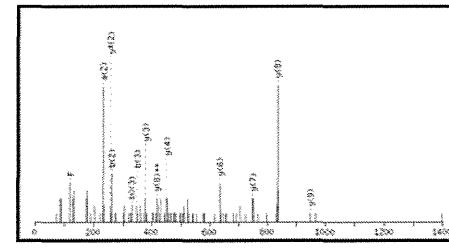

FISLGEACKK , Start – End Sequence: 713 - 722

Fig. 1 **a** Partially purified proteins were separated by SDS–PAGE using serum samples from HCV-HCC patients. The Coomassie-stained SDS-PAGE gel shows two clear bands at approximately 8 kDa (*X* and *Y*). **b** After each band (*X* and *Y*) was excised from the gel, the proteins were extracted and analyzed using the ProteinChip system. The target protein in the excised band was detected, and the 8.1 k m/z peak corresponded only to the "*Y*" band contained in gel. **c** The excised "*Y*" band was alkylated and digested using trypsin. The peptides were collected and subjected to LC–MS/MS analysis. The proteins, which were derived from complement C3a, were identified using a database search

was reduced. On the other hand, immunodepletion with a control anti-C4 antibody or without antibody did not reduce the 8.1 k m/z peak (Fig. 2).

Profiling the C3a of sera from patients with HCC and without HCC

The 8.1 k m/z peak was confirmed as the complement C3a fragment using an immunodepletion assay. However, C3a was stabilized as C3adesArg with a molecular weight of approximately 8.9 k m/z. Figure 3a, b compares the expression of the 8.1 k m/z peak in the sera of HCV-HCC or HCV-CLD patients and healthy controls. The intensities in HCC patient sera were significantly higher than those in the HCV-CLD patients or healthy controls. The expression of the 8.9 k m/z peak in HCV-HCC patients was also higher than that in HCV-CLD patients or healthy controls (Fig. 3c, d). Although the 8.9 k m/z peak was not identified as C3adesArg, it is possible that both the 8.1 and 8.9 k m/z peaks were specific tumor markers for HCC. Furthermore, we analyzed sera from 10 HCV-HCC patients who were diagnosed with HCC within 1 or 2 years and sera from five patients who had received curative treatments using RFA, PEIT, and TACE for HCC. The 8.1 k m/z C3a fragment in the HCV-HCC patients was significantly increased in the year of disease onset compared to the pre-onset year. After treatment, expression of the C3a fragment significantly decreased in all five of the patients who had measurable samples after treatment (Fig. 4a). In contrast, the 8.9 k m/z peak did not change regardless of the occurrence of HCC over time (Fig. 4b). Thus, the 8.1 k m/z C3a fragment appears to be the most discriminatory tumor marker for HCV-HCC.

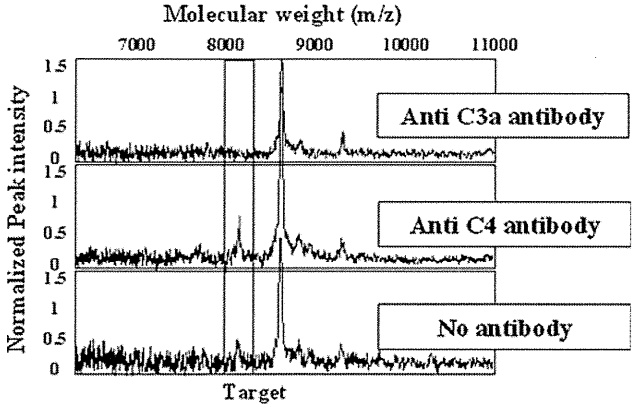

Fig. 2 Immunodepletion assay of the C3a fragment. Analysis of supernatant that had been immunodepleted with an anti-C3a antibody showed that only the 8.1 k m/z peak corresponding to complement C3a was reduced. Supernatants that had been immunodepleted with either a control anti-C4 antibody or without antibody did not have reduced 8.1 k m/z peaks by the ProteinChip system

Relationship between the C3a fragment and other tumor markers

AFP and DCP levels were measured in sera from 83 of 87 patients with HCV-associated liver disease. The recommended cutoff levels for these tumor markers, AFP and DCP, are 20 ng/ml and 40 mAU/ml, respectively. AFP-L3 in 26 patients with HCV-associated liver disease was also investigated among measurable samples in which AFP in a total 35 patients was higher than 20 ng/ml. The cutoff level of AFP-L3 was set at 10%. When samples from patients

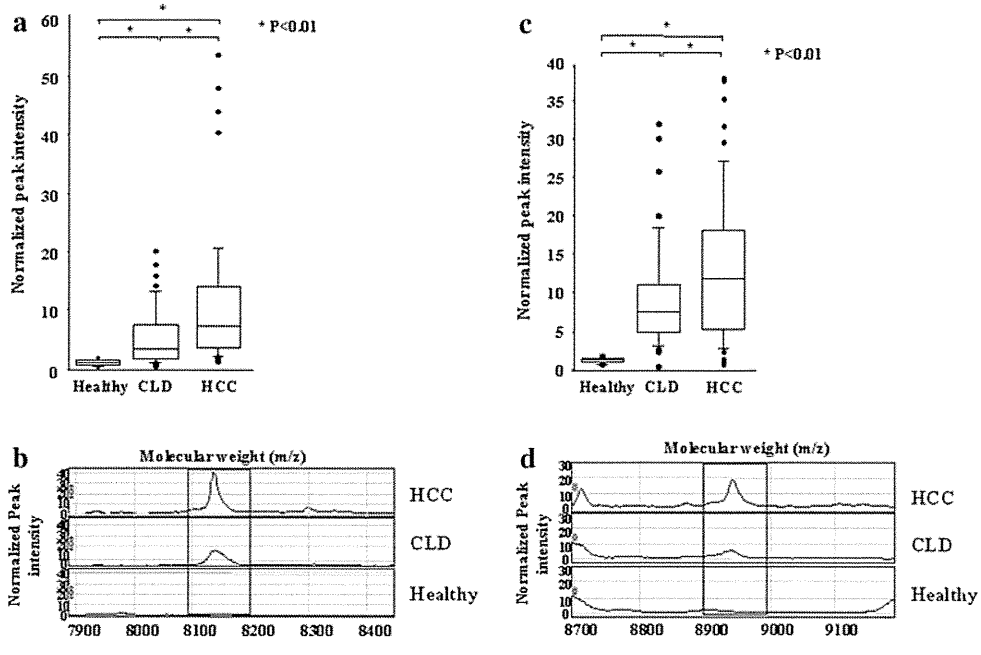

Fig. 3 **a** and **c** Comparisons of the expression profiles of the 8.1 and 8.9 k m/z peaks in HCV-HCC, HCV-CLD, and healthy sera. *Boxes* indicate the median ± 25th percentile. The *lower* and *upper bars* represent the 10th and 90th percentiles, respectively. **b** and **d** Representative spectra of the 8.1 and 8.9 k m/z peaks from patients in each group. The *horizontal axis* indicates the protein molecular weight, while the *vertical axis* designates the relative intensity

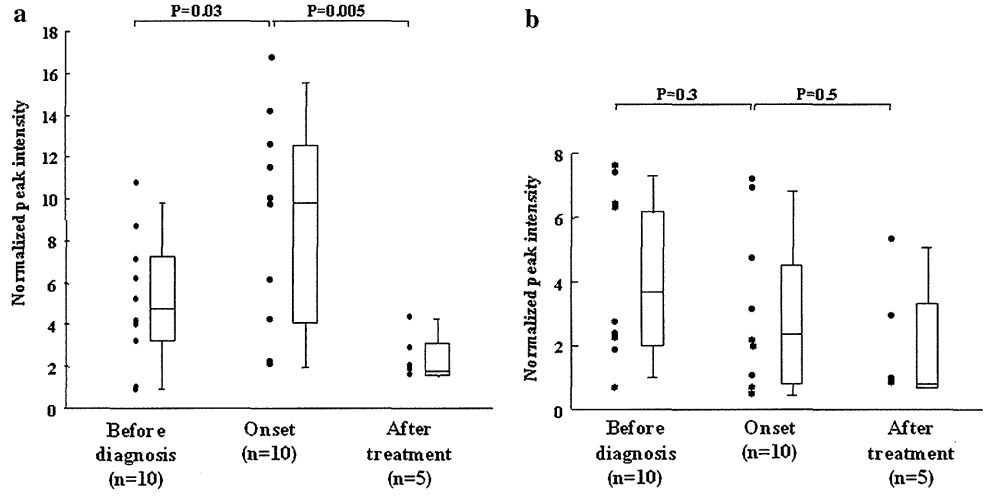

Fig. 4 Comparisons of the expression profiles of the 8.1 k m/z (**a**) and 8.9 k m/z (**b**) peaks in sera from HCV-HCC patients before diagnosis, during disease onset, and after treatment. The samples in the before diagnosis group included sera collected 1 or 2 years before the onset of HCC. *Boxes* indicate the median ± 25th percentile, the *lower bar* indicates the 10th percentile and the *upper bar* indicates the 90th percentile

Table 2 Diagnostic rates for hepatocellular carcinoma in the HCV infected patients

Markers	Sensitivity (%)	Specificity (%)	ROC AUC
AFP[a] (>20 ng/ml)	38 (17/45)	47 (18/38)	0.53
DCP[b] (>40 mAU/ml)	45 (20/44)	74 (29/39)	0.68
AFP-L3[c] (>10%)	58 (8/14)	50 (6/12)	0.58
C3a fragment (>3.5)	78 (37/45)	52 (22/42)	0.70
C3a fragment + AFP	91 (41/45)	26 (10/38)	0.72
C3a fragment + DCP	93 (41/44)	33 (13/39)	0.77
AFP + DCP	64 (28/44)	34 (12/35)	0.70
C3a fragment + AFP + DCP	98 (43/44)	20 (7/35)	0.80

[a] Alpha fetoprotein

[b] Des-γ-carboxy prothrombin

[c] Alpha fetoprotein, lectin lens culinaris agglutin-bound fraction

with HCV-HCC and HCV-CLD without HCC were compared, the sensitivity and specificity of AFP were 38 and 47%, whereas those of DCP were 45 and 74% and those of AFP-L3 were 58 and 50%, respectively. When the cutoff level for the relative intensity of the C3a fragment was set at 3.5, the sensitivity and specificity were 78 and 52%, respectively; the C3a fragment had the most sensitivity for the diagnosis of HCC. Furthermore, the ROC AUC of the C3a fragment, AFP, DCP, and AFP-L3 was 0.70, 0.53, 0.68, and 0.58, respectively (Table 2). There was no relationship between the C3a fragment and several other tumor and inflammation markers [AFP, DCP, AFP-L3, alanine aminotransferase (ALT), and high-sensitivity C-reactive protein (hs-CRP)], and each of these markers was independent of the diameter and number of tumors. The ROC AUC using AFP and DCP was highly similar to the ROC AUC with the C3a fragment alone. In addition, we investigated a combination assay that included the C3a fragment, AFP and DCP. This combination test, in which at least AFP, DCP, or the C3a fragment was positive, had a positive identification rate of 98%, although the specificity of this assay was too low at 20%. The ROC AUC of the combination test using AFP, DCP, and the C3a fragment was higher than those of any other markers. This result indicates that this combination assay using three markers is more useful than the combination assay using AFP ± DCP, which are measured worldwide to detect HCC (Table 2).

Profiling C3a expression in culture medium

C3a reacted with HCC cell lines, and the C3a peak in the culture medium was monitored by the ProteinChip system. The C3a fragment (approximately 8.1 k m/z) was not detected in the supernatants of HuH-7 and HepG2 cell cultures. However, the 8.9 k m/z peak was detected in the culture medium. This 8.9 k m/z peak was considered to be a stabilized form of C3a. This result indicated that the stabilized form of C3a (8.9 k m/z) was not undergoing proteasome-mediated degradation to yield the C3a fragment (8.1 k m/z) in these HCC cell lines.

Discussion

Because the HCC disease-associated mortality rate remains high, it is highly important to develop early diagnostic tools and treatments for HCC. Our study indicates that an 8.1 k m/z peak, which was identified as the C3a fragment by both peptide sequencing and an immunoassay, is up-regulated in the serum of HCC patients, 93% (42/45) of whom were TNM stage I or II. The C3a fragment in some HCC cases was also significantly higher in the year of HCC onset compared to the pre-onset year and decreased after curative treatment. Therefore, the C3a fragment appears to

be a promising simple tumor marker for the diagnosis of early HCC. In addition, a combination serum HCC diagnostic test that included AFP, DCP, and the C3a fragment had higher sensitivity than each individual marker. These results suggest that this combination test may be a useful HCC screening method, although the low specificity may pose challenges. Further examinations are needed to determine whether the C3a fragment or a combination test can be used to detect early HCC.

The results of our study demonstrated that the C3a fragment (8.1 k m/z) is a highly expressed novel tumor marker that is abundant in the sera of early HCC patients but not in the sera of healthy volunteers or HCV-CLD patients. A similar study by Lee et al. [17] used the ProteinChip SELDI system to show that C3a is a potential candidate biomarker for HCV-HCC. However, Lee et al. found that the molecular weight of C3a was represented by an approximately 8.9 k m/z peak. C3a has a very short half-life and is immediately cleaved into the more stable C3adesArg (8.9 k m/z), which is the anaphylatoxin C3a that lacks the C-terminal arginine and is stable state in the serum [23]. In our study, the 8.9 k m/z peak was also significantly different among HCV-HCC patients, HCV-CLD patients, and healthy volunteers (Fig. 3c, d). However, the discriminatory power of the 8.9 k m/z peak (ROC AUC was 0.60) was lower than the 8.1 k m/z peak (ROC AUC was 0.70) to distinguish between HCV-HCC and HCV-CLD. In addition, unlike the 8.1 k m/z peak, the levels of the 8.9 k m/z peak did not significantly increase with time as HCC progressed in 10 HCV-HCC cases (Fig. 4b). In contrast, Li et al. identified two proteins (8926 m/z and 8116 m/z) as complement component C3adesArg and a C-terminal truncated form of C3adesArg; the latter was a C-terminal truncation of C3adesArg that lacked the C-terminal sequence RASHLGLA (referred to as C3adesArgΔ8) in breast cancer patients [24]. However, these two biomarkers cannot be used to discriminate between breast cancers and benign tumors, and there were minimal differences in the peak intensities between breast cancer patients and healthy controls. Therefore, the C3a fragment with a molecular weight of 8.1 k m/z appears to be a potential diagnostic marker for HCC, although we cannot explain why the 8.1 k m/z fragment of C3a is overexpressed in HCC patients and did not confirm whether our C3a fragment (8.1 k m/z) is C3adesArgΔ8.

C3a, including C3adesArg, was also previously identified as a tumor marker for lymphoid malignancies, breast and colorectal cancers using the ProteinChip SELDI system [24–26]. Complement activation and subsequent deposition of complement components on tumor tissues has been demonstrated in cancer patients [27]. Malignant ovarian cells isolated from ascitic fluid samples had C3 activation products deposited on their cell surface [28]. Complement components are important mediators of inflammation and help regulate the immune response. C3a is biologically active and binds to mast cells and basophils, triggering the release of their vasoactive contents [29]. We investigated C3a expression by immunochemical examination of HCC tissues and Western blot analysis of proteins extracted from human HCC cell lines, including HepG2 and HuH-7. However, specific C3a expression, including the C3a fragment (8.1 k m/z), was not detected.

The complement system can be activated after exposure to tumor antigens [30]. It is speculated that small tumors can trigger a systematic reaction. Therefore, elevated C3a (8.9 k m/z) levels in the serum of HCV-HCC patients may reflect both a systematic immune response to HCV infection and non-specific tumor antigens rather than a specific immune response to HCC [24–26, 31]. In contrast, it is possible that overexpression of the C3a fragment (8.1 k m/z) is specific for HCC in addition to non-specific C3 activation.

In contrast to our results, Steel et al. [32] searched for HCC biomarkers using HCC-associated HBV-infected patient sera and found that the C-terminal fragment of complement C3 was down-regulated. Kawakami et al. [33] searched for characteristic alterations in the sera of HBV- and HCV-HCC-infected patients who had undergone curative radiofrequency ablation treatment and showed that C3 was up-regulated after treatment. In these studies, C3 was separated and identified using 2-DE of a mixture of proteins from a small number of patient sera samples, and this process identified various molecular weights for C3. In addition, we analyzed the sera of 25 patients with HCC-associated HBV infections, and the profile of several proteins was different between HCV- and HBV-infected patients. Although 35 protein peaks, including the C3a fragment, were overexpressed in the sera of both HCV-HCC and HBV-HCC patients compared to sera from healthy volunteers, the C3a fragment (8.1 k m/z) was particularly overexpressed in the sera of HCV-HCC patients and was not significantly different between HBV-HCC patients and HCV-CLD patients without HCC (data not shown). The biologic and pathogenic activities of HCV and HBV are different, and the molecular mechanisms underlying the development of hepatitis and hepatocarcinogenesis may differ between HBV and HCV infections [34–36]. Although the number of samples, cause of liver disease, and method of protein identification may affect these results, we speculate that the C3a fragment with a molecular weight of 8.1 k m/z is a candidate tumor marker for HCV-HCC but not HBV-HCC.

AFP, which is a commonly used HCC tumor marker, is elevated not only during HCC, but also during hepatocyte regeneration following liver damage. Previous reports revealed that AFP was abnormally elevated in the sera of patients with acute hepatitis, chronic hepatitis, and liver

cirrhosis. This lack of specificity for HCC means that AFP has a comparatively high false-positive rate [37]. The C3a fragment may also be elevated during hepatocyte regeneration following liver damage [38], and early diagnosis of small HCC tumors may be difficult with one marker alone. Therefore, the false-positive rates for HCC must be carefully considered [39–41]. Also, a combination of markers, including AFP, DCP, and the C3a fragment, in the serum should be verified to improve the diagnostic rate.

The ProteinChip SELDI system can separate and partially characterize multiple proteins in tissue and serum samples. Our previous report used a panel of proteins to diagnose early HCC with the ProteinChip SELDI system [15]. This panel diagnosis of seven protein peaks included a discriminant peak of 4060 m/z. This 4060 m/z peak may be a double-charged 8130 m/z peak, although the C3a fragment (8130 m/z) was not used to develop this diagnostic method. These results suggest that the C3a fragment is a useful HCC biomarker, regardless of whether this fragment carries a single or double charge. In addition, the panel diagnosis method is more useful than measuring the C3a fragment alone to diagnose and predict the occurrence of HCC. However, this method must be performed using the ProteinChip SELDI system, which is expensive and does not detect putative interactions between various proteins. Identifying a specific HCC protein such as the C3a fragment will also further our understanding of the molecular mechanisms of hepatocarcinogenesis. Therefore, the C3a fragment should not only be considered a simple HCC tumor marker, but should also be evaluated for its contribution to HCC carcinogenesis.

In conclusions, serum profiling with the ProteinChip SELDI system may be used to distinguish HCC from chronic liver disease without HCC and to detect early HCC in HCV-infected patients. Because we identified the C3a fragment (8.1 k m/z) in serum samples from HCC patients, the C3a fragment is a promising marker that can be used to screen for HCV-HCC and to develop new therapeutic targets.

Acknowledgments We thank Mr. Hiroyuki Nakao for assistance with the statistical analyses. We also thank Ms. Yuko Morinaga for her technical assistance. This work was supported in part by a grant-in-aid from the Collaboration of Regional Entities for the Advancement of Technological Excellence (CREATE) from the Japan Science and Technology Agency, a grant (no. CA87982) from the United States National Institutes of Health, and a grant-in-aid (Research on Hepatitis and BSE) from the Ministry of Health, Labour and Welfare of Japan.

References

1. El-Serag HB, Mason AC. Rising incidence of hepatocellular carcinoma in the United States. N Engl J Med. 1999;340:745–50.
2. Robert GG. Hepatocellular carcinoma: overcoming challenges in disease management. Clin Gastroenterol Hepatol. 2006;4:252–61.
3. Okuda K. Hepatocellular carcinoma. J Hepatol. 2000;32:225–37.
4. Oka H, Tamori A, Kuroki T, Kobayashi K, Yamamoto S. Prospective study of alpha-fetoprotein in cirrhotic patients monitored for development of hepatocellular carcinoma. Hepatology. 1994;19:61–6.
5. Ishii M, Gama H, Chida N, Ueno Y, Shinzawa H, Takagi T, et al. Simultaneous measurements of serum alpha-fetoprotein and protein induced by vitamin K absence for detecting hepatocellular carcinoma. South Tohoku District Study Group. Am J Gastroenterol. 2000;95:1036–40.
6. Okuda H, Nakanishi T, Takatsu K, Saito A, Hayashi N, Takasaki K, et al. Serum levels of des-gamma-carboxy prothrombin measured using the revised enzyme immunoassay kit with increased sensitivity in relation to clinicopathologic features of solitary hepatocellular carcinoma. Cancer. 2000;88:544–9.
7. Grazi GL, Mazziotti A, Legnani C, Jovine E, Miniero R, Gallucci A, et al. The role of tumor markers in the diagnosis of hepatocellular carcinoma, with special reference to the des-gamma-carboxy prothrombin. Liver Transpl Surg. 1995;1:249–55.
8. Wang CS, Lin CL, Lee HC, Chen KY, Chiang MF, Chen HS, et al. Usefulness of serum des-gamma-carboxy prothrombin in detection of hepatocellular carcinoma. World J Gastroenterol. 2005;11:6115–9.
9. Marrero JA, Su GL, Wei W, Emick D, Conjeevaram HS, Fontana RJ, et al. Des-gamma carboxyprothrombin can differentiate hepatocellular carcinoma from nonmalignant chronic liver disease in American patients. Hepatology. 2003;37:1114–21.
10. Mita Y, Aoyagi Y, Yanagi M, Suda T, Suzuki Y, Asakura H. The usefulness of determining des-gamma-carboxy prothrombin by sensitive enzyme immunoassay in the early diagnosis of patients with hepatocellular carcinoma. Cancer. 1998;82:1643–8.
11. Taketa K, Okada S, Win N, Hlaing NK, Wind KM. Evaluation of tumor markers for the detection of hepatocellular carcinoma in Yangon General Hospital, Myanmar. Acta Med Okayama. 2002;56:317–20.
12. Khien VV, Mao HV, Chinh TT, Ha PT, Bang MH, Lac BV, et al. Clinical evaluation of lentil lectin-reactive alpha-fetoprotein-L3 in histology-proven hepatocellular carcinoma. Int J Biol Markers. 2001;16:105–11.
13. Zinkin NT, Grall F, Bhaskar K, Otu HH, Spentzos D, Kalmowitz B, et al. Serum proteomics and biomarkers in hepatocellular carcinoma and chronic liver disease. Clin Cancer Res. 2008;14:470–7.
14. Schwegler EE, Cazares L, Steel LF, Adam BL, Johnson DA, Semmes OJ, et al. SELDI-TOF MS profiling of serum for detection of the progression of chronic hepatitis C to hepatocellular carcinoma. Hepatology. 2005;41:634–42.
15. Kanmura S, Uto H, Kusumoto K, Ishida Y, Hasuike S, Nagata K, et al. Early diagnostic potential for hepatocellular carcinoma using the SELDI ProteinChip system. Hepatology. 2007;45:948–56.
16. Paradis V, Degos F, Dargère D, Pham N, Belghiti J, Degott C, et al. Identification of a new marker of hepatocellular carcinoma by serum protein profiling of patients with chronic liver diseases. Hepatology. 2005;41:40–7.
17. Lee IN, Chen CH, Sheu JC, Lee HS, Huang GT, Chen DS, et al. Identification of complement C3a as a candidate biomarker in human chronic hepatitis C and HCV-related hepatocellular carcinoma using a proteomics approach. Proteomics. 2006;6:2865–73.
18. Uto H, Hayashi K, Kusumoto K, Hasuike S, Nagata K, Kodama M, et al. Spontaneous elimination of hepatitis C virus RNA in individuals with persistent infection in a hyperendemic area of Japan. Hepatol Res. 2006;34:28–34.
19. Shevchenko A, Wilm M, Vorm O, Mann M. Mass spectrometric sequencing of proteins silver-stained polyacrylamide gels. Anal Chem. 1996;68:850–8.
20. Prahalad AK, Hickey RJ, Huang J, Hoelz DJ, Dobrolecki L, Murthy S, et al. Serum proteome profiles identifies parathyroid hormone physiologic response. Proteomics. 2006;6:3482–93.

21. Shiwa M, Nishimura Y, Wakatabe R, Fukawa A, Arikuni H, Ota H, et al. Rapid discovery and identification of a tissue-specific tumor biomarker from 39 human cancer cell lines using the SELDI ProteinChip platform. Biochem Biophys Res Commun. 2003;309:18–25.
22. Adam BL, Qu Y, Davis JW, Ward MD, Clements MA, Cazares LH, et al. Serum protein fingerprinting coupled with a pattern-matching algorithm distinguishes prostate cancer from benign prostate hyperplasia and healthy men. Cancer Res. 2002;62: 3609–14.
23. Sahu A, Lambris JD. Structure and biology of complement protein C3, a connecting link between innate and acquired immunity. Immunol Rev. 2001;180:35–48.
24. Miguet L, Bogumil R, Decloquement P, Herbrecht R, Potier N, Mauvieux L, et al. Discovery and identification of potential biomarkers in a prospective study of chronic lymphoid malignancies using SELDI-TOF-MS. J Proteome Res. 2006;5:2258–69.
25. Ward DG, Suggett N, Cheng Y, Wei W, Johnson H, Billingham LJ, et al. Identification of serum biomarkers for colon cancer by proteomic analysis. Br J Cancer. 2006;94:1898–905.
26. Li J, Orlandi R, White CN, Rosenzweig J, Zhao J, Seregni E, et al. Independent validation of candidate breast cancer serum biomarkers identified by mass spectrometry. Clin Chem. 2005;51:2229–35.
27. Jurianz K, Ziegler S, Garcia-Schüler H, Kraus S, Bohana-Kashtan O, Fishelson Z, et al. Complement resistance of tumor cells: basal and induced mechanisms. Mol Immunol. 1999;36:929–39.
28. Bjørge L, Hakulinen J, Vintermyr OK, Jarva H, Jensen TS, Iversen OE, et al. Ascitic complement system in ovarian cancer. Br J Cancer. 2005;92:895–905.
29. Mollnes TE, Garred P, Bergseth G. Effect of time, temperature and anticoagulants on in vitro complement activation: consequences for collection and preservation of samples to be examined for complement activation. Clin Exp Immunol. 1988;73: 484–8.
30. Verhaegen H, De Cock W, De Cree J, Verbruggen F. Increase of serum complement levels in cancer patients with progressing tumors. Cancer. 1976;38:1608–13.
31. Habermann JK, Roblick UJ, Luke BT, Prieto DA, Finlay WJ, Podust VN, et al. Increased serum levels of complement C3a anaphylatoxin indicate the presence of colorectal tumors. Gastroenterology. 2006;131:1020–9.
32. Steel LF, Shumpert D, Trotter M, Seeholzer SH, Evans AA, London WT, et al. A strategy for the comparative analysis of serum proteomes for the discovery of biomarkers for hepatocellular carcinoma. Proteomics. 2003;3:601–9.
33. Kawakami T, Hoshida Y, Kanai F, Tanaka Y, Tateishi K, Ikenoue T, et al. Proteomic analysis of sera from hepatocellular carcinoma patients after radiofrequency ablation treatment. Proteomics. 2005;5:4287–95.
34. Honda M, Kaneko S, Kawai H, Shirota Y, Kobayashi K. Differential gene expression between chronic hepatitis B and C hepatic lesion. Gastroenterology. 2001;120:955–66.
35. Kim W, Oe Lim S, Kim JS, Ryu YH, Byeon JY, Kim HJ, et al. Comparison of proteome between hepatitis B virus- and hepatitis C virus-associated hepatocellular carcinoma. Clin Cancer Res. 2003;9:5493–500.
36. Koike K. Steatosis, liver injury, and hepatocarcinogenesis in hepatitis C viral infection. J Gastroenterol. 2009;44:82–8.
37. Lok AS, Lai CL. Alpha-fetoprotein monitoring in Chinese patients with chronic hepatitis B virus infection: role in the early detection of hepatocellular carcinoma. Hepatology. 1989;9:110–5.
38. Markiewski MM, Mastellos D, Tudoran R, DeAngelis RA, Strey CW, Franchini S, et al. C3a and C3b activation products of the third component of complement (C3) are critical for normal liver recovery after toxic injury. J Immunol. 2004;173:747–54.
39. Oka H, Kurioka N, Kim K, Kanno T, Kuroki T, Mizoguchi Y, et al. Prospective study of early detection of hepatocellular carcinoma in patients with cirrhosis. Hepatology. 1990;12:680–7.
40. Tanaka N, Horiuchi A, Yamaura T, Komatsu M, Tanaka E, Kiyosawa K. Efficacy and safety of 6-month iron reduction therapy in patients with hepatitis C virus-related cirrhosis: a pilot study. J Gastroenterol. 2007;42:49–55.
41. Tsamandas AC, Antonacopoulou A, Kalogeropoulou C, Tsota I, Zabakis P, Giannopoulou E, et al. Oval cell proliferation in cirrhosis in rats. An experimental study. Hepatol Res. 2007;37:755–64.

Hepatology Research

Hepatology Research 2012 doi: 10.1111/hepr.12032

Original Article

Serum RANTES level influences the response to pegylated interferon and ribavirin therapy in chronic hepatitis C

Kazuki Komase,[1] Shinya Maekawa,[1,2] Mika Miura,[1] Ryota Sueki,[1] Makoto Kadokura,[1] Hiroko Shindo,[1] Kuniaki Shindo,[1] Fumitake Amemiya,[1] Yasuhiro Nakayama,[1] Taisuke Inoue,[1,2] Minoru Sakamoto,[1] Atsuya Yamashita,[3] Kohji Moriishi[3] and Nobuyuki Enomoto[1]

[1]*First Department of Medicine, Faculty of Medicine,* [2]*Department of Advanced Medicine for Liver Diseases, Faculty of Medicine, and* [3]*Department of Microbiology, University of Yamanashi, Yamanashi, Japan*

Aim: Prediction of treatment responses to pegylated interferon (PEG IFN) plus ribavirin (RBV) therapy is uncertain for genotype 1b chronic hepatitis C.

Methods: In this study, 96 patients were investigated for the correlation between 36 pretreatment serum chemokine/cytokine levels and PEG IFN/RBV treatment efficacy by a sandwich enzyme-linked immunoassay (ELISA) and a bead array.

Results: First, chemokines/cytokines were measured semi-quantitatively by sandwich ELISA in 31 randomly-selected patients and the serum regulated on activation normal T-cell expressed and secreted (RANTES) level was found to be significantly higher in the sustained virological response (SVR) group than the non-SVR group ($P = 0.048$). Precise RANTES measurement in all 96 patients using a bead array confirmed this correlation ($P = 0.002$). However, the genetic RANTES haplotype was not significantly related to the serum level. The serum RANTES level was extracted by multivariate analysis (odds ratio = 4.09, 95% confidence interval = 1.02–16.5, $P = 0.048$) as an independent variable contributing to SVR.

Conclusion: The serum RANTES level is an important determinant influencing the virological response to PEG IFN/RBV therapy in chronic hepatitis C.

Key words: hepatitis C virus, pegylated interferon plus ribavirin therapy, RANTES

INTRODUCTION

HEPATITIS C VIRUS (HCV) is a major cause of chronic liver disease worldwide and persistent infection may lead to liver cirrhosis and hepatocellular carcinoma.[1] Therapy leading to HCV eradication is the only treatment with proven efficacy in decreasing the occurrence of hepatocellular carcinoma.[2] Recently, treatment with telaprevir, a non-structural (NS)3/4A protease inhibitor, combined with pegylated interferon (PEG IFN) and ribavirin (RBV), increased the rates of sustained viral response (SVR) up to 64–75%[3,4] compared to the SVR rate of approximately 50% for the previous PEG IFN/RBV therapy. However, it has become evident that genotype 1-infected patients with a null response to previous PEG IFN/RBV therapy have poor responses to PEG IFN/RBV/telaprevir,[5] with an SVR rate as low as approximately 30%, illustrating the difficulty in treating patients infected with genotype 1 HCV. Therefore, precise and accurate prediction of the viral response to PEG IFN/RBV therapy remains an important issue.

Treatment resistance is attributed to various factors associated with the virus and host. Viral factors, such as amino acid (a.a.) sequence variation in the core and NS5A regions, have been investigated extensively for their contribution to the outcome of IFN-based therapy,[6,7] including PEG IFN/RBV therapy. On the other hand, host factors such as African-American race, older age, being obese, the presence of cirrhosis and

Correspondence: Dr Shinya Maekawa, First Department of Medicine, Faculty of Medicine, University of Yamanashi, 1110 Shimokato, Chuo, Yamanashi 409-3898, Japan. Email: maekawa@yamanashi.ac.jp

Conflict of interest: Shinya Maekawa and Taisuke Inoue belong to a donation-funded department that is funded by MSD (Tokyo, Japan). Nobuyuki Enomoto received research funding from MSD (Tokyo, Japan) and Roche (Tokyo, Japan).

Received 26 September 2012; revision 18 November 2012; accepted 26 November 2012.

steatosis, and insulin resistance have been reported to be associated with treatment resistance.[8–11] Especially, single nucleotide polymorphisms (SNP) near the interleukin (*IL*)-28B gene, including rs12979860 and rs8099917, have been reported to have a significant correlation with the response to IFN-based therapy.[12,13] However, even with inclusion of these factors, prediction of the treatment response in chronic HCV infection remains uncertain at present.

Chemokines are a group of small, exogenously secreted cytokines that modulate the migration of leukocytes to sites of tissue damage and inflammation in a variety of infectious and autoimmune diseases.[14] In chronic HCV infection, chemokines such as *RANTES* (regulated on activation normal T-cell expressed and secreted), macrophage inflammatory protein (*MIP*)-1α, *MIP-1β* and interferon-γ inducible protein 10 kDa (*IP-10*) are elevated and considered to play crucial roles in inflammatory processes and viral elimination, as well as the transition from innate to adaptive immunity.[14,15] Upregulation of several serum chemokines, such as eotaxin, *IP-10* and *RANTES* also has been reported in HCV infection, possibly reflecting hepatic inflammation.[16] Considering the roles of chemokines/cytokines in establishing chronic hepatitis, it is possible that these chemokines also affect the response to antiviral therapy, and actually several chemokines as interleukin (*IL*)-8, *IL-10*, *MIP-1β*, *RANTES* or *IP-10* have been investigated previously for their association with the treatment response.[16–20] However, the importance of those chemokines has not been established yet and, moreover, these studies did not characterize in detail these chemokines in association with other factors, including *IL-28B* influencing the response to therapy.

In this study, we explored extensively the association of 36 serum cytokines/chemokines and the treatment response, with detailed information of host and virus, to predict better the treatment response to PEG IFN and RBV therapy in genotype 1b HCV infection. Because the pretreatment serum *RANTES* level was found to be correlated significantly with the response, we analyzed further the association between the serum level of *RANTES* and the genomic SNP.

METHODS

Patients

NINETY-SIX CONSECUTIVE PATIENTS with genotype 1b HCV and receiving PEG IFN/RBV therapy between 2004 and 2010 at Yamanashi University Hospital were recruited retrospectively into the study. All patients received the standard therapy according to the treatment protocol of PEG IFN/RBV therapy for Japanese patients, established by a hepatitis study group of the Ministry of Health, Labor and Welfare, Japan (PEG IFN-α-2b 1.5 μg/kg bodyweight, once weekly s.c., and RBV 600–800 mg daily p.o. for 48 weeks).[21] All patients enrolled fulfilled the following criteria: (i) negative for hepatitis B surface antigen; (ii) no other forms of hepatitis, such as primary biliary cirrhosis, autoimmune liver disease or alcoholic liver disease; (iii) not co-infected with HIV; and (iv) a signed consent was obtained for the study protocol that had been approved by the Human Ethics Review Committee of Yamanashi University Hospital. The study was approved by the ethics committees of University of Yamanashi, and the study protocol conformed to the ethical guidelines of the 2008 Declaration of Helsinki.

Definition of treatment outcome

An SVR was defined as undetectable serum HCV RNA at 24 weeks after the end of treatment. Relapse was defined as reappearance of detectable HCV RNA levels following discontinuation of treatment. Null response was defined as less than 2 log decrease of the baseline HCV RNA levels after 12 weeks of treatment. Based on this definition, when patients were classified according to the achievement of SVR, patients with relapse or null response were classified as non-SVR.

Serum cytokine measurement

Sandwich enzyme-linked immunosorbent assay (ELISA)

Blood samples were collected before initiation of treatment and were stored at −80°C until use. Semiquantitation of serum cytokines was performed using the Proteome Profiler Human Cytokine Array Kit Panel A (R&D Systems, Minneapolis, CA, USA) according to the manufacturer's instructions. The kit consists of a nitrocellulose membrane containing 36 different anti-cytokine antibodies (anti-C5a, anti-CD154, anti-G-CSF, anti-GM-CSF, anti-CXCL1, anti-CCL1, anti-sICAM-1, anti-IFN-γ, anti-IL-1α, anti-IL-1β, anti-IL-1ra, anti-IL-2, anti-IL-4, anti-IL-5, anti-IL-6, anti-IL-8, anti-IL-10, anti-IL-12p70, anti-IL-13, anti-IL-16, anti-IL-17, anti-IL-17E, anti-IL-23, anti-IL-27, anti-IL-32α, anti-IP-10, anti-CXCL11, anti-CCL2, anti-MIF, anti-CCL3, anti-CCL4, anti-PAI-1, anti-RANTES, anti-CXCL12, anti-TNF-α, anti-sTREM-1), spotted in duplicate. Serum samples were diluted and mixed with a cocktail of biotinylated detection antibodies. The sample/antibody mixture

was then incubated with the membrane. Any cytokine/detection antibody complex present was bound to the membrane by its cognate immobilized capture antibody. Following washing to remove unbound material, streptavidin-horseradish peroxidase and chemiluminescent detection reagents (ECL Western Blotting Analysis System; GE Healthcare, Buckinghamshire, UK) were added sequentially. Arrays were scanned using a LAS-3000 mini-luminescent image analyzer (Fujifilm, Tokyo, Japan) and were quantified for the densities using Multi Gauge ver. 3.0 software (Fujifilm). Concentrations of cytokines and chemokines were expressed as their signal intensity ratios relative to that of the positive control spotted on the same membrane.

Bead array

Precise serum concentrations of regulated on *RANTES* were measured using the Luminex Bio-Plex system (Bio-Rad, Hercules, CA, USA) and the Procarta Cytokine Assay Kit (Panomics, Fremont, CA, USA) in a 96-well plate ELISA-based format according to the manufacturers' recommendations. The sensitivity of the assays is greater than 10 pg/mL cytokine. Serum and standards were incubated with a mixture of the Luminex antibody-conjugated beads for 30 min with constant shaking. After washing, the detection antibodies and substrates were added and incubated for another 30 min. Fluorescent signals were collected and data expressed, using internal standards, in pg/mL as the mean of two individual experiments carried out in duplicate.

Viral core and interferon sensitivity-determining region (ISDR) sequence determination by direct sequencing

Hepatitis C virus RNA extraction from serum samples, complementary DNA synthesis and amplification by two-step nested polymerase chain reaction (PCR) were carried out using specific primers for the HCV core and ISDR. PCR amplicons were sequenced directly by Big Dye Terminator ver. 3.1 (ABI, Tokyo, Japan) with universal M13 forward and reverse primers using an ABI prism 3130 sequencer (ABI). The sequence files generated were assembled using Vector NTI software (Invitrogen, Tokyo, Japan) and base-calling errors were corrected following inspection of the chromatogram.

SNP typing of the *RANTES* and *IL-28B* genes

Genomic DNA of the patients was extracted from peripheral blood using a blood DNA extraction kit (QIAGEN, Tokyo, Japan) according to the manufacturer's protocol. The allele typing of each DNA sample was performed by real-time PCR with a model 7500 (ABI) using FAM-labeled SNP primers for the loci rs2107538, rs2280788, rs2280789, rs4796120 and rs3817655 (ABI) for *RANTES* and the locus rs8099917 (ABI) for IL-28B.

Statistical analysis

Student's *t*-test and Mann–Whitney *U*-test were used to analyze continuous variables, as appropriate. Fisher's exact test was used for the analysis of categorical variables. Receiver–operator curve (ROC) analyses were performed to establish cut-off values for serum cytokine concentration. The optimum cut-off was defined as the value that maximized the area under the ROC. Spearman's correlation coefficient (R) was calculated to clarify the strength of relationship between the pretreatment serum cytokine concentrations and clinical parameters. Variables that achieved statistical significance ($P < 0.05$) in univariate analysis were entered into multiple logistic regression analysis to identify significant independent factors. The odds ratios and 95% confidence intervals also were calculated. Data were analyzed using Ekuseru-Toukei 2008 (SSRI, Tokyo, Japan). The haplotype block among rs2107538, rs2280788, rs2280789, rs4796120 and rs3817655 variants was analyzed using SNPAlyze software ver. 8.0 (Dynacom, Chiba, Japan). $P < 0.05$ was considered significant.

RESULTS

Semiquantitative measurement of pretreatment serum cytokines in 31 randomly-selected patients

AT FIRST, TO identify cytokines/chemokines related to the treatment responses to PEG IFN/RBV therapy, semiquantitative measurement of the serum concentrations of 36 comprehensive cytokines/chemokines was performed by sandwich ELISA method by randomly selected patients. Next, to further confirm the result, cytokines showing the associations with the response were measured more precisely by bead array method in all patients.

In the first analysis, 31 patients were randomly selected from the 96 patients. The clinical characteristics of these 31 patients at the start of the therapy are shown in Table 1. Significant differences in the clinical backgrounds between those who did and those who did not

Table 1 Baseline characteristics of the 31 patients analyzed using the sandwich ELISA method

Factor	SVR ($n = 20$)	Non-SVR ($n = 11$)	*P*-value
Age (years)	52 ± 11†	57 ± 10	0.25‡
Sex (male : female)	11:9	6:5	0.64§
Bodyweight (kg)	60.9 ± 9.6†	61.9 ± 13.9	0.81‡
Body mass index (kg/m^2)	22.6 (18.9–31.3)¶	22.7 (17.5–26.8)	0.87††
History of IFN therapy (%)	30	36	0.78§
ALT (IU/L)	130 ± 100†	75 ± 35	0.09‡
AST (IU/L)	76 (22–331)¶	64 (24–178)	0.73††
γ-GTP (IU/L)	40 (12–289)	52 (24–137)	0.17††
Albumin (g/dL)	4.1 (3.7–4.5)	4.0 (3.0–4.7)	0.46††
Total cholesterol (mg/dL)	170 ± 24†	149 ± 33	0.06‡
HbA1c (%)	5.3 ± 0.5	5.3 ± 0.6	0.95‡
Creatinine (mg/dL)	0.71 ± 0.15	0.68 ± 0.15	0.54‡
WBC count (/μL)	4561 ± 1631	4056 ± 1277	0.38‡
Neutrophil count (/μL)	2130 (820–4200)¶	1500 (800–2700)	0.02††
Hemoglobin (g/dL)	14.5 ± 1.0†	13.8 ± 1.6	0.15‡
Platelet count (×10^{-4}/μL)	16.4 ± 5.4	12.2 ± 3.9	0.03‡
α-Fetoprotein (ng/mL)	4.6 (1.4–28.9)¶	22.3 (11.4–79.7)	0.00005††
HCV RNA (KIU/mL)	1520 ± 1079†	2146 ± 899	0.11‡
Fibrosis (F1/F2/F3/F4)‡‡	14/1/1/2	3/2/2/3	0.02††
Activity (A1/A2/A3)‡‡	12/5/1	3/5/2	0.06††

†Mean ± standard deviation.
‡Student's *t*-test.
§Fisher's exact probability test.
¶Median (range).
††Mann–Whitney *U*-test.
‡‡SVR, $n = 18$; non-SVR, $n = 10$.
Activity, the score of activity in liver biopsies; ALT, alanine aminotransferase; AST, aspartate aminotransferase; ELISA, enzyme-linked immunoassay; fibrosis, the score of fibrosis in liver biopsies; HbA1c, hemoglobin A1c; HCV, hepatitis C virus; SVR, sustained virological response; WBC, white blood cell; γ-GTP, γ-glutamyl transpeptidase.

achieve SVR were neutrophil counts, platelet counts, serum α-fetoprotein levels and the score of fibrosis in liver biopsies. Table 2 shows the difference in the cytokine/chemokine expression between the SVR and the non-SVR group. Because some cytokines/chemokines were below the measurement limit of the ELISA kit, as shown in Table 1, those cytokine/chemokines were not studied further. As shown here, the *RANTES* level was significantly higher in the SVR group than the non-SVR group ($P = 0.048$).

Precise measurement of serum *RANTES* in all 96 patients

Because the semiquantitative measurement of pretreatment serum *RANTES* levels in 31 randomly selected patients demonstrated their significant correlation with the SVR, we determined the precise serum RANTES levels in all 96 patients using the bead array method and investigated the correlation between those concentrations and the treatment outcome. The clinical characteristics of the 96 patients are shown in Table 3. Significant differences were seen between those with and without SVR in platelet count, viral loads and the liver fibrosis score, but there was no apparent difference in the total doses of PEG IFN and RBV. As shown in Figure 1, the distribution of serum *RANTES* levels in each treatment response differed significantly; the median serum *RANTES* level in the SVR group was significantly higher than that in the non-SVR group. Successive ROC analysis confirmed a significant association of the serum *RANTES* level with SVR, and the cut-off value of 3400 pg/mL to be most appropriate (Table 4). Using the cut-off value of 3400 pg/mL, 50.9% sensitivity, 79.5% specificity, 78.4% positive predictive value and 52.5% negative predictive value (area under the ROC, 0.643) were obtained for the prediction of SVR by serum *RANTES* level.

Table 2 Difference in cytokine and chemokine expression between the SVR group and the non-SVR group in the 31 patients

Cytokine/chemokine	SVR ($n = 20$)	Non-SVR ($n = 11$)	*P*-value
RANTES	4.99 (0.25–8.32)†	1.24 (0.17–8.01)	0.048‡
MIF	1.31 (0.06–3.31)†	0.45 (0.08–2.67)	0.0630
IL-1ra	0.09 (0.00–3.30)†	0.07 (0.00–2.05)	0.2300
PAI-1	3.10 (0.35–7.34)†	2.73 (0.46–8.42)	0.3900
sICAM-1	3.18 (0.37–8.33)†	2.78 (0.74–10.3)	0.4800
IL-23	0.08 (0.01–0.78)†	0.07 (0.00–0.38)	0.5900
IL-27	0.05 (0.02–0.18)†	0.05 (0.00–0.23)	0.6500
IL-6	0.08 (0.01–3.22)†	0.10 (0.00–1.36)	0.7100
C5a	0.21 (0.01–2.72)†	0.12 (0.00–1.67)	0.7700
IFN-γ	0.07 (0.02–0.31)†	0.08 (0.00–0.40)	0.8000
CCL4	0.04 (0.01–3.08)†	0.05 (0.00–0.69)	0.8400
IL-32α	0.04 (0.00–0.71)†	0.07 (0.00–0.20)	0.9000
IL-8	0.16 (0.05–2.61)†	0.17 (0.03–2.21)	0.9300
IL-1α			N.A.
IL-1β			N.A.
IL-2			N.A.
IL-4			N.A.
IL-5			N.A.
IL-10			N.A.
IL-12 p70			N.A.
IL-13			N.A.
IL-16			N.A.
IL-17			N.A.
IL-17E			N.A.
CCL1			N.A.
CCL2			N.A.
CCL3			N.A.
CXCL1			N.A.
CXCL11			N.A.
CXCL12			N.A.
CD154			N.A.
G-CSF			N.A.
GM-CSF			N.A.
IP-10			N.A.
TNF-α			N.A.
sTREM-1			N.A.

†Median (range).
‡Mann–Whitney *U*-test.
N.A., not available; SVR, sustained virological response.

Correlation between serum *RANTES* level and clinical parameters

Spearman's correlation coefficients between the pre-treatment serum *RANTES* level and clinical parameters in all 96 patients are shown in Table 5. As a result, a significant negative correlation with aspartate aminotransferase level and a significant positive correlation with platelet count were found, while no significant correlation was observed in other clinical parameters.

Univariate and multivariate analysis of factors related to SVR

Univariate and multivariate analyses were performed successively in order to clarify the factors related to SVR. The viral factors included in the analysis were the ISDR and core a.a. 70 and 91, along with the host factor, IL-28B SNP. Those factors, conventional clinical background factors and serum *RANTES* levels were subjected to univariate and multivariate analysis. In the univariate

Table 3 Baseline characteristics of all patients analyzed using the bead array method ($n = 96$)

Factor	SVR ($n = 57$)	Non SVR ($n = 39$)	*P*-value
Age (years)	53 ± 10†	57 ± 8	0.08‡
Sex (male : female)	34:23	23:16	0.56§
Bodyweight (kg)	60.6 ± 10.5†	57.8 ± 7.8	0.17‡
Body- mass index (kg/m^2)	22.9 ± 2.8	22.1 ± 2.2	0.15‡
History of IFN therapy (%)	25	28	0.74§
ALT (IU/L)	68 (19–413)¶	64 (20–215)	0.25††
AST (IU/L)	58 (21–331)	62 (21–178)	0.80††
γ-GTP (IU/L)	37 (11–289)	50 (13–167)	0.12††
Albumin (g/dL)	4.1 ± 0.3†	4.1 ± 0.4	0.93‡
Total cholesterol (mg/dL)	166 ± 30	158 ± 31	0.25‡
HbA1c (%)	5.2 (4.7–6.6)¶	5.3 (4.5–7.4)	0.47††
Creatinine (mg/dL)	0.72 ± 0.15†	0.69 ± 0.16	0.39††
WBC count (/μL)	4497 ± 1247	4501 ± 1281	0.99‡
Neutrophil count (/μL)	2243 ± 857	2144 ± 825	0.57‡
Hemoglobin (g/dL)	14.1 ± 1.2	14.2 ± 1.2	0.87‡
Platelet count (×10^{-4}/μL)	15.1 (7–29)¶	13.2 (6.9–19.7)	0.03††
α-Fetoprotein (ng/mL)	4.8 (1.3–137.1)	9.0 (1.4–79.7)	0.05††
HCV RNA (KIU/mL)	1300 (100–5000)	2400 (620–5000)	0.0002‡
Fibrosis (F1/F2/F3/F4)‡‡	35/6/5/6	11/13/5/6	0.006††
Activity (A1/A2/A3)‡‡	27/18/7	12/20/3	0.26††
PEG IFN dose (%)	92 (40–113)¶	73 (27–147)	0.23††
RBV dose (%)	97 (44–147)	100 (33–135)	0.38††

†Mean ± standard deviation.
‡Student's *t*-test.
§Fisher's exact probability test.
¶Median (range).
††Mann–Whitney's *U*-test.
‡‡SVR, $n = 52$; non-SVR, $n = 35$.
Activity, the score of activity in liver biopsies; ALT, alanine aminotransferase; AST, aspartate aminotransferase; fibrosis, the score of fibrosis in liver biopsies; HbA1c, hemoglobin A1c; HCV, hepatitis C virus; PEG IFN, pegylated interferon; RBV, ribavirin; SVR, sustained virological response; WBC, white blood cell; γ-GTP, γ-glutamyl transpeptidase.

analysis, significant differences were observed for the ISDR mutation, core a.a. 70, viral loads, platelet counts, IL-28B SNP and serum *RANTES* levels. When multivariate analysis was carried out with these factors, the serum RANTES level was extracted as an independent factor related to SVR (Table 6).

RANTES haplotyping and serum *RANTES* level

Because a high serum *RANTES* level was an independent factor predicting SVR, we sought to examine further the role of the RANTES gene and tried to clarify the association of the SNP of the gene with the serum levels. First, we determined how many and which SNP in the *RANTES* gene should be investigated to represent all *RANTES* haplotypes found in the Japanese population. Reference to the HapMap project database (http://snp.cshl.org) made it clear that the information from five unique SNP was required to determine the majority of haplotypes found in the Japanese population. Therefore, to determine the *RANTES* haplotype of each patient, we investigated these five SNP in the 65 of the 96 patients available for the haplotype analysis. The *RANTES* haplotypes were finally divided into three types (named R1, R2 and R3 for convenience), as shown in Figure 2(a). However, the *RANTES* gene haplotype and serum RANTES level did not show any clear correlation (Fig. 2b).

DISCUSSION

FROM THE ANALYSIS of 36 cytokine and chemokine species, we discovered that a high pretreatment serum *RANTES* level was significantly related to SVR